Chapter 23

Predicting Chaos

We have discussed methods for diagnosing chaos, but what about predicting the existence of chaos in a dynamical system. This is a much harder problem, and it seems that the best that can be done is to predict the existence of "chaotic sets" that are not attractors but may perhaps "organize" the chaotic attractor. These methods rely on the understanding of the complicated structure that emerges in phase space when a homoclinic or heteroclinic orbit is perturbed. To introduce these ideas we first introduce a definition of chaos that is useful for sets that are not attractors, motivating the idea using the simplest of chaotic maps, the shift map.

23.1 The Shift Map and Symbolic Dynamics

The map

$$x_{n+1} = 2x_n \bmod 1 \tag{23.1}$$

displays many of the features of chaos in an analytically accessible way. The tent map at $a = 2$ is equivalent to the shift map.

To understand the dynamics write the initial point in binary representation $x_0 = 0.a_1 a_2 \ldots$ equivalent to

$$x_0 = \sum a_v 2^{-v} \tag{23.2}$$

with each a_i either 0 or 1. The action of the map is simply to shift the "binal" point to the right and discard the first digit

$$x_1 = f(x_0) = 0.a_2 a_3 \ldots \tag{23.3}$$

Many properties are now evident:

1. Sensitivity to initial conditions: two initial conditions differing by of order 2^{-m} lead to orbits that differ by $O(1)$ after m iterations.

2. The answer to the question whether the mth iteration from a random initial condition is greater or less than $\frac{1}{2}$ is as random as a coin toss. This reduction of chaotic dynamics to a random sequence of 0 and 1 (called a Bernouilli sequence) by a fixed partition of the phase space is known as "symbolic dynamics".

3. Information is created at 1 bit per iteration (the Kolmogorov entropy).

4. There are a countable infinity of initial conditions (those with x_0 rational) that lead to (unstable) periodic orbits. The complement of this set is of measure 1 i.e. most initial conditions lead to chaotic orbits.

Presumably these properties of the binary shift were known well before the modern study of chaos. Indeed this example seems to reduce the phenomena of chaos to a trivial reflection of the choice of initial condition. The change of perspective in the past few decades is that this map is indeed a trivial example, but an example representative of a phenomenon that occurs in physical systems and one that remains hard to understand in general.

23.2 Alternative Definition of Chaos

An alternative definition of chaos that also applies to sets that are not attractors is:

> A deterministic dynamics is chaotic if for any prescribed Bernouilli sequence we can find an initial state for which the dynamics will reproduce the sequence as it moves through a fixed partition of the phase space.

This definition does not require that the "chaotic motion" be an attractor, and so is more useful mathematically than physically.
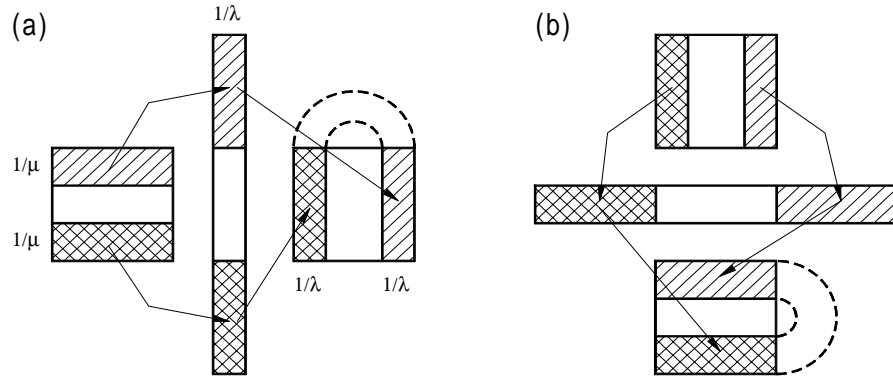
Figure 23.1: Construction of (a) the Horseshoe map and (b) the inverse map.

23.3 Smale Horseshoe

Consider the map M of the unit square D given by figure (23.1a), with parameters λ and μ. Note that we are only interested in points that are mapped back into the square: the "horseshoe" connection is only used to illustrate the continuity. After one iteration portions of the unit square are mapped to two vertical stripes of width λ^{-1} that we will label V_0 and V_1. Successive iterations lead to finer and finer stripes (figure 23.2a). The inverse map can be constructed in a similar manner, figure (23.1b). Iterating the inverse map on the unit square leads to finer and finer horizontal stripes (figure 23.2a). Note that

$$M(H_0) = V_0 \quad \text{and} \quad M^{-1}(V_0) = H_0 \tag{23.4}$$
$$M(H_1) = V_1 \quad \text{and} \quad M^{-1}(V_1) = H_1$$

Under each forward or backward iteration some points will be mapped outside the square and are no longer considered, i.e. the measure of the set decreases at each iteration and eventually, after a large number of iterations, almost all initial conditions will leave the square, i.e. the generated set is not an attractor. However we may construct the invariant set Λ that is invariant under an arbitrary number of iterations:

$$\ldots M^{-2}(D) \cap M^{-1}(D) \cap D \cap M(D) \cap M^2(D) \cap \ldots \tag{23.5}$$
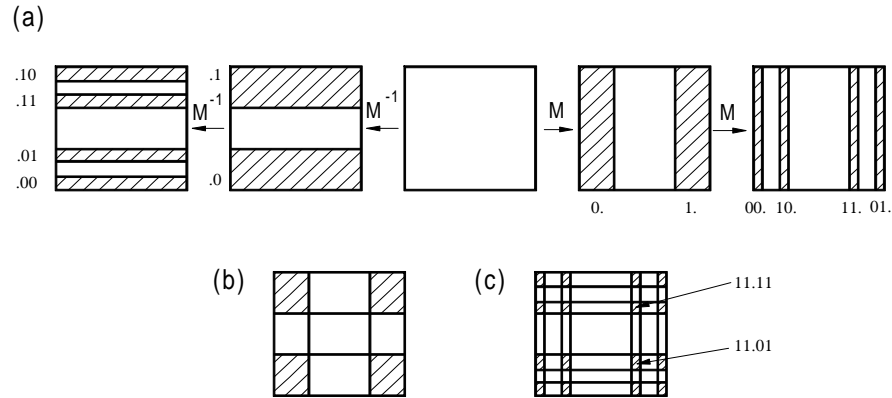
Figure 23.2: (a) Iterates of the map and the inverse on the unit square. The labelling of the vertical stripes should be read backwards from the decimal point, the labelling of horizontal stripes forwards. Then the labels show the horizontal or vertical location now and at previous iterates of M (vertical) or M^{-1} (horizontal). (b) and (c): constructing the invariant set, first and second level.

The first two levels of this construction $M^{-1}(D) \cap D \cap M(D)$ and $M^{-2}(D) \cap M^{-1}(D) \cap D \cap M(D) \cap M^2(D)$ are shown in figure (23.2): the regions left in the set can be labelled by a bi-infinite sequence of 0's and 1's corresponding to the horizontal and vertical striping. The labels can be combined into a binary number (vertical indices).(horizontal indices)

$$\vec{x} \equiv \dots s_{-2}s_{-1} \cdot s_0 s_1 s_2 \dots \tag{23.6}$$

where

$$s_i = \begin{cases} 0 & \text{if} \quad M^i(\vec{x}) \text{ is in } H_0 \\ 1 & \text{if} \quad M^i(\vec{x}) \text{ is in } H_1 \end{cases}. \tag{23.7}$$

The effect of the map is then $M(\vec{x}) = \vec{x}'$ where $\vec{x}'$ is given by shifting the "binal" point one step to the right. Thus again a dynamical system is reduced to the binary shift operation (but in the present case, the horseshoe map is invertible, unlike the shift map above). Again this means that periodic orbits are dense in Λ (start from an initial point represented by a periodic binary expansion), but there are an

uncountable number of nonperiodic orbits (irrational initial conditions), and there is at least one orbit that is dense in Λ (i.e. comes arbitrarily close to any point).

Note the similarity to the bakers' map construction. The Smale horseshoe has the advantage of being continuous. On the other hand the invariant set is not an attractor, and is reached only for a set of initial conditions in the square of measure zero. However because the map is smooth, we have the chance of finding it in smooth dynamical systems, so that non-attracting chaotic sets can be proven to occur on these cases. Often there are nearby attracting chaotic sets, although the connection between these two phenomena does not seem to be understood.

23.4 Homoclinic Tangles

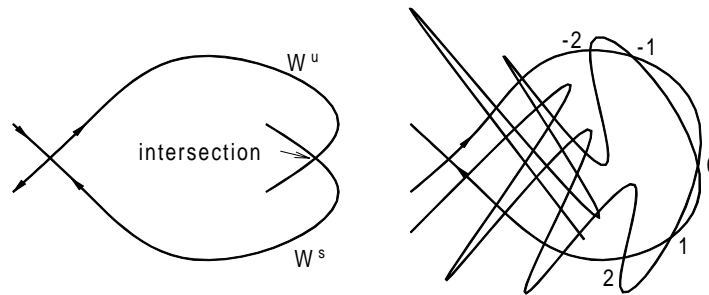### 23.4.1 Stable and unstable manifolds

Figure 23.3: Homoclinic Tangle

Consider a fixed point in an invertible 2-dimensional map M with one stable and one unstable direction. The *stable* and *unstable manifolds* of the fixed point x_f were introduced in chapter 22: the stable manifold of x_f is the set of points $\vec{x}$ such $M^n \vec{x} \to \vec{x}_f$ as $n \to \infty$; the unstable manifold of x_f is the set of points $\vec{x}$ such $M^{-n} \vec{x} \to \vec{x}_f$ as $n \to \infty$. The stable and unstable manifolds are the nonlinear extension of the stable and unstable eigenvectors of the linear analysis around $\vec{x}_f$. The existence and smoothness of the manifolds is proven under quite general conditions. Although the manifolds are curves, the dynamics of the map from one initial condition will, of course, jump between discrete points on the curve.

The stable manifold cannot cross itself or the stable manifold of another fixed point (since then there would be a point without a unique inverse). Similarly an unstable manifold cannot cross itself or another unstable manifold. However an unstable manifold can cross a stable manifold. When this occurs through a transverse intersection rather than a tangency, a "homoclinic tangle" (or "heteroclinic tangle" if the manifolds belong to different fixed points) occurs, and it can be shown that a Smale horseshoe is produced, so that chaotic dynamics occurs (but need not be an attractor).

The construction is shown in figure (23.3). Suppose the manifolds intersect at the point $\vec{x}_0$, which therefore lies both on the stable manifold W^s and the unstable manifold W^u. The map $\vec{x}_1 = M(\vec{x}_0)$ of $\vec{x}_0$ must also lie on both W^u and W^s and so is another intersection of the manifolds. There are an infinite number of points $M^n(\vec{x}_0)$ before the fixed point $\vec{x}_f$ is reached, and so there are an infinite number of intersections. As the point $M^n(\vec{x}_0)$ approaches $\vec{x}_f$ the unstable manifold is stretched along the unstable direction, but in a way that cannot lead to self intersections. Similarly under the inverse mapping M^{-n} an infinite number of intersections are produced. This gives the wild type of behavior shown in figure (23.3)
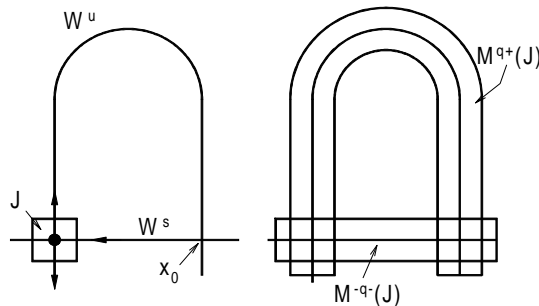

Figure 23.4: Horseshoe due to a homoclinic intersection.

Now consider the effect of the map on a small square J centered on the fixed point. The map will stretch the square along W^u (using continuity and the fact that the fixed point remains fixed). After a sufficient number q_+ of forward iterations $J^+ = M^{q_+}(J)$ will include the intersection point $\vec{x}_0$. Similarly under inverse iterations J is stretched along W^s and after a sufficient number q_- of iterations $J^- = M^{-q_-}(J)$ will include the point $\vec{x}_0$. Now if we look at the effect of the map

$\bar{M} = M^{q_+ + q_-}$ on J^- we find that $\bar{M}$ is the horseshoe map! Thus the transverse intersection of W^u and W^s implies the existence of complex dynamics.
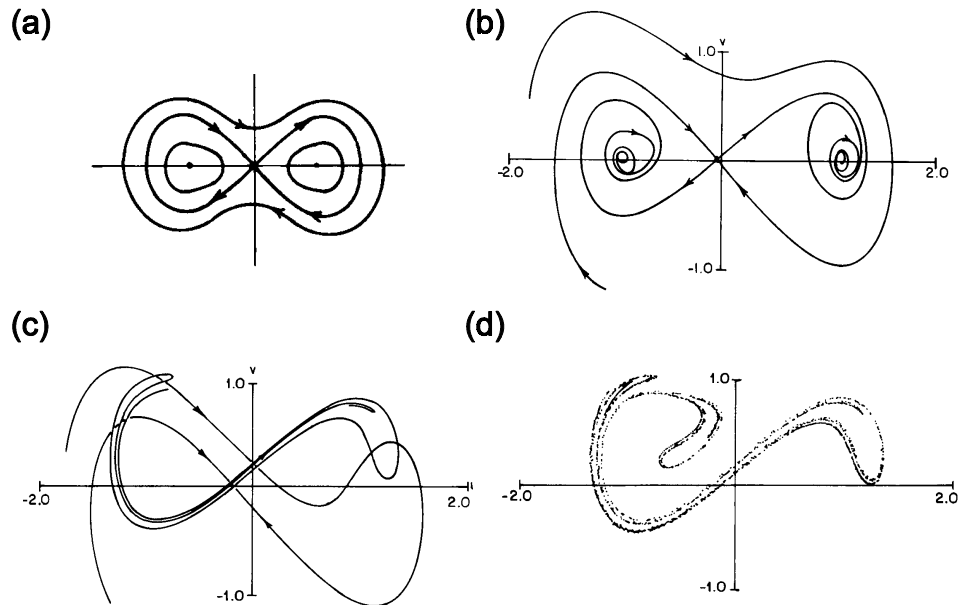

Figure 23.5: Poincare section for Duffing Oscillator: (a) driving strength $g = 0$ and no damping $\gamma = 0$; (b) stable and unstable manifolds for $g = 0.10$; (c) stable and unstable manifolds for $g = 0.40$; (d) attractor for $g = 0.40$. In (b)-(d) the damping is $\gamma = 0.25$ and the drive freqeuncy is $\omega_D = 1$. (From Guckenheimer and Holmes)

The Duffing oscillator (chapter 3) illustrates these ideas [2]. Consider $\omega_D = 1$ and $\gamma = 0.25$. For small driving $g = 0.1$ the unstable manifold of the fixed point $(0,0)$ spirals into one or other of the stable fixed points and the Poincaré section plot reproduces the phase plane plot for no driving. As g increases an intersection of W^s and W^u occurs leading to the homoclinic tangle. The numerical plot of the chaotic attractor seems to coincide with W^u (see the plots in figure 23.5 at $g = 0.4$).
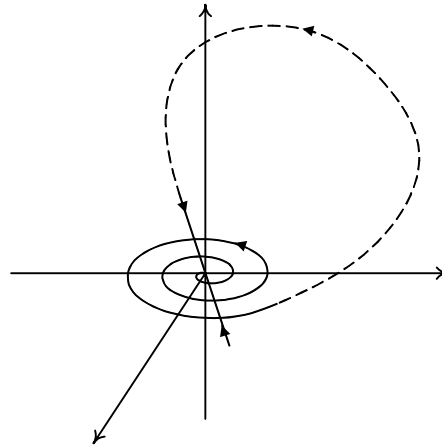
Figure 23.6: Geometry of Silnikov chaos

23.5   Silnikov Chaos

Consider a homoclinic orbit in a three dimensional phase space at a fixed point
with a complex pair of unstable eigenvalues σ and σ^* and a real stable eigenvalue
λ (figure 23.6). If there is a homoclinic orbit and also the condition $|\operatorname{Re}\sigma| < |\lambda|$
is satisfied, then Silnikov showed that there are horseshoes and thus chaos in the
return map defined near the homoclinic orbit (see Guckenheimer and Holmes [2],
section 6.5). The same result applies for $\operatorname{Re}\sigma < 0$ (spiralling in) and $\lambda > 0$. The
Rossler map (see Odes demonstrations) appears to mimic this structure.

February 20, 2000

Bibliography

[1] K.T. Aligood, T.D. Sauer, and J.A. Yorke, "Chaos: an Introduction to Dynamical Systems" (Springer 1997)

[2] J. Guckenheimer and P. Holmes, "Nonlinear Oscillations, Dynamical Systems, and Bifurcations of Vector Fields" (Springer, 1983).